environments

MDPI

*Article*

# Hydrochemical Characteristics and Spatial Patterns of Shallow Groundwater Contamination in a Lowland Settlement in Hungary

**Tamás Mester [1,*], Mária Vasvári [1], Dániel Balla [2] and Tibor Kovács [3]**

[1] Department of Landscape Protection and Environmental Geography, University of Debrecen, 4032 Debrecen, Hungary; vasvari.maria@science.unideb.hu
[2] Department of Data Science and Visualization, Faculty of Informatics, University of Debrecen, 4028 Debrecen, Hungary; balla.daniel@inf.unideb.hu
[3] Institute of Rural Development and Sustainable Economy, Hungarian University of Agriculture and Life Sciences, 2100 Gödöllő, Hungary; kovacs.tibor@uni-mate.hu
* Correspondence: mester.tamas@science.unideb.hu

## Abstract

Shallow groundwater contamination remains a major environmental challenge in urban–agricultural environments, where multiple sources of pollution and natural hydrogeochemical processes contribute to pronounced spatial variability in groundwater quality. This study aimed to characterize the hydrochemical properties, spatial patterns of contamination, and potential pollution sources of shallow groundwater in Kisújszállás, Hungary. Groundwater levels and physicochemical parameters were investigated in 24 residential dug wells in autumn 2026, with complete hydrochemical datasets available for 22 wells. Field and laboratory measurements were assessed using correlation analysis, hierarchical cluster analysis (HCA), principal component analysis (PCA), and GIS-based spatial interpolation and land use assessment. Groundwater elevations ranged from 80.14 to 84.57 m a.s.l., while groundwater depths varied between 0.46 and 5.72 m. Considerable hydrochemical variability was observed, with EC ranging from 367 to 8460 µS/cm, $NO_3^-$ from 0.131 to 1233.28 mg/L, and $Cl^-$ from 22.73 to 2236.39 mg/L. Spatial analysis revealed localized areas of elevated concentrations, particularly in the northeastern and central-southern areas. HCA identified three distinct groundwater groups characterized by contrasting salinity, nutrient enrichment, and redox conditions. The spatial distribution of the HCA-derived clusters showed possible association with land-use categories, with differences between the built-up area, enclosed garden areas, and agricultural surroundings. PCA revealed that the first three components explained 82.38% of the total variance, supporting the identification of distinct hydrochemical patterns. The $NO_3^-$/$Cl^-$ relationships suggested overlapping influences of domestic wastewater, household gardening, agricultural activities, and natural salinization. These findings contribute to effective groundwater management in lowland settlements and highlight the need for seasonal groundwater monitoring and the inclusion of additional wells selected to improve the representation of different land-use categories.

**Keywords:** groundwater contamination; urban–agricultural environment; domestic wastewater; nitrate; GIS; land use; multivariate statistical analysis; groundwater level

Academic Editor: Melida Gutierrez

Received: 21 October 2026
Revised: 15 November 2026
Accepted: 23 November 2026
Published: 24 November 2026

**Copyright:** © 2026 by the authors. Licensee MDPI, Basel, Switzerland. This article is an open access article distributed under the terms and conditions of the Creative Commons Attribution (CC BY) license.

## 1. Introduction

Shallow groundwater in urban and peri-urban environments is particularly vulnerable to anthropogenic contamination due to intensive land use, urban infrastructure, and various domestic and agricultural activities [1,2]. Its hydrochemical composition reflects the combined influence of natural processes and human-induced pressures, frequently resulting in pronounced spatial variability within relatively small areas [3–5]. Major contamination sources include domestic wastewater, leaking sewer networks, on-site sanitation systems, agricultural inputs, and urban runoff, which may introduce nutrients, dissolved salts, organic compounds, and microbial contaminants into shallow aquifers [6,7]. Numerous studies have highlighted the importance of non-agricultural contamination sources in urban groundwater systems, demonstrating that multiple anthropogenic activities can substantially contribute to groundwater deterioration [8–10]. Similarly, Schirmer et al. emphasized the complex interactions among urban land use, groundwater recharge, contaminant transport, and subsurface biogeochemical processes [11]. These findings underline the importance of integrated hydrochemical investigations for understanding groundwater quality and identifying potential contamination pathways in municipal environments.

Domestic wastewater constitutes a major source of shallow groundwater contamination, particularly in settlements with inadequate sanitation infrastructure [12,13]. Leakage from unsealed cesspits, septic systems, and defective sewer networks may introduce nutrients, dissolved salts, organic matter, and microbial contaminants into the subsurface [14]. Robertson et al. investigated two septic-system plumes in shallow sandy aquifers in Canada and documented elevated concentrations of nitrate, chloride, and dissolved organic carbon, with one contamination plume extending more than 130 m downgradient from the source [15]. In Germany, a nationwide assessment estimated that sewer exfiltration contributed 9.8% and 17.2% of nitrate and phosphate emissions from urban wastewater systems, respectively [16]. Comparable concerns have been documented in the Hungarian Great Plain, where Mester et al. identified substantial nitrate contamination prior to the construction of the sewerage network and demonstrated that elevated concentrations persisted in several monitoring wells during the subsequent monitoring period [17]. These findings emphasize the long-term implications of wastewater infiltration and the importance of groundwater monitoring in municipal environments.

Nitrate ($NO_3^-$) and phosphate ($PO_4^{3-}$) are frequently associated with anthropogenic groundwater contamination, particularly in areas affected by domestic wastewater, agricultural activities, and inadequate sanitation [18–20]. Similar groundwater quality problems have been documented across diverse geographical and hydrogeological settings worldwide. In peri-urban communities near Accra, Ghana, Annan et al. reported elevated nitrate and phosphate concentrations in wells located within 30 m of septic tanks, indicating the influence of inadequate wastewater disposal [21]. In Urânia, Brazil, Hirata et al. documented persistent nitrate contamination despite the development of sewerage infrastructure, with concentrations exceeding 120 mg/L in the oldest urbanized areas [22]. Comparable problems have been identified in Central Europe. In western Poland, Dragon et al. reported nitrate concentrations reaching 72 mg/L in shallow groundwater affected by agricultural activities and settlements with incomplete sewerage coverage [23]. Similarly, a study in the Hungarian Great Plain revealed persistent nutrient contamination more than a decade after sewerage network development, with a median nitrate concentration of 108.9 mg/L and frequent phosphate exceedances [24]. These findings highlight the widespread occurrence of nutrient contamination and the importance of local pollution sources and hydrogeochemical conditions. Furthermore, the combined assessment of nutrient concentrations, dissolved oxygen (DO), oxidation–reduction potential (ORP),

and chemical oxygen demand (COD) provides complementary information on groundwater redox conditions and potential biogeochemical transformations [25,26].

Chloride ($Cl^-$) is widely used as a hydrochemical indicator of anthropogenic groundwater contamination, particularly in areas affected by domestic wastewater, septic systems, and agricultural activities [27,28]. Katz et al., evaluating groundwater chemistry in more than 2000 wells across the United States, demonstrated that elevated chloride concentrations, combined with chloride-to-bromide ratios and other chemical indicators, can provide evidence of septic-system impacts on shallow aquifers [29]. Similarly, a study in the South Bengal Basin, India, identified wastewater-related groundwater contamination through elevated chloride concentrations and characteristic ionic ratios [30]. However, high chloride concentrations may also occur naturally in saline and salt-affected environments, where evaporation, shallow groundwater fluctuations, and the accumulation of soluble salts contribute to groundwater salinization. In the Great Hungarian Plain, Tóth et al. demonstrated a strong relationship between shallow groundwater conditions and the spatial distribution of salt-affected soils [31]. Furthermore, de Craats et al. highlighted the role of capillary rise and evapotranspiration in salt accumulation in the Hortobágy region [32]. Consequently, elevated chloride concentrations in shallow groundwater should not be interpreted exclusively as evidence of wastewater contamination, particularly in lowland areas characterized by saline or sodic soils [33].

Comprehensive groundwater quality assessments are essential for understanding the combined effects of municipal wastewater, agricultural activities, and local hydrogeochemical conditions, particularly in shallow aquifers underlying lowland settlements. The present study therefore investigates the spatial variability of shallow groundwater quality in Kisújszállás, a settlement in the Great Hungarian Plain, Hungary, characterized by a residential core, enclosed gardens, agricultural surroundings, shallow groundwater, and salt-affected soils occurring in close proximity. By integrating physicochemical and nutrient-related parameters, groundwater-level observations, multivariate statistical analyses, and GIS-based spatial assessment, the study aims to identify distinct hydrochemical groundwater groups, characterize spatial contamination patterns, and examine potential anthropogenic influences. Particular attention is given to nitrogen species, chloride enrichment, and redox conditions to provide an integrated assessment of shallow groundwater quality in a municipal environment.

The settlement provides a case study of a broader problem affecting lowland settlements, where residential and agricultural pressures coexist with naturally salt-affected soils. Unlike earlier studies by this research group focusing primarily on wastewater-related changes over time [17,24], the present investigation emphasizes small-scale hydrochemical heterogeneity through the combined assessment of groundwater levels, chemical parameters, multivariate patterns, and land use.

## 2. Materials and Methods

### *2.1. Study Area*

The study was conducted in Kisújszállás (Figure 1), an urban settlement in Jász-Nagykun-Szolnok County, in the central part of the Great Hungarian Plain, Hungary, with a population of approximately 10,200 inhabitants (2026). The settlement is characterized by a predominantly residential built-up area surrounded by extensive agricultural land, reflecting historical landscape transformations driven by agricultural activities, river regulation, and water management interventions that reduced the extent of natural water bodies and expanded cultivated areas [34]. The area belongs to the Szolnok–Túr Plain microregion, characterized by a nearly level alluvial landscape with elevations ranging from approximately 80 to 105 m above sea level [35]. The spatial distribution of surface

elevations within the administrative boundaries of Kisújszállás is illustrated by the digital elevation model (DEM) presented in Figure 1.

Municipal wastewater management, agricultural activities, and industrial operations are important environmental factors that may influence groundwater quality in Kisújszállás. The municipal sewerage network covers the entire urban area, and approximately 90% of residential properties were connected to the system by 2012. Furthermore, local building regulations require properties with access to the public sewerage network to be connected to the system [36].

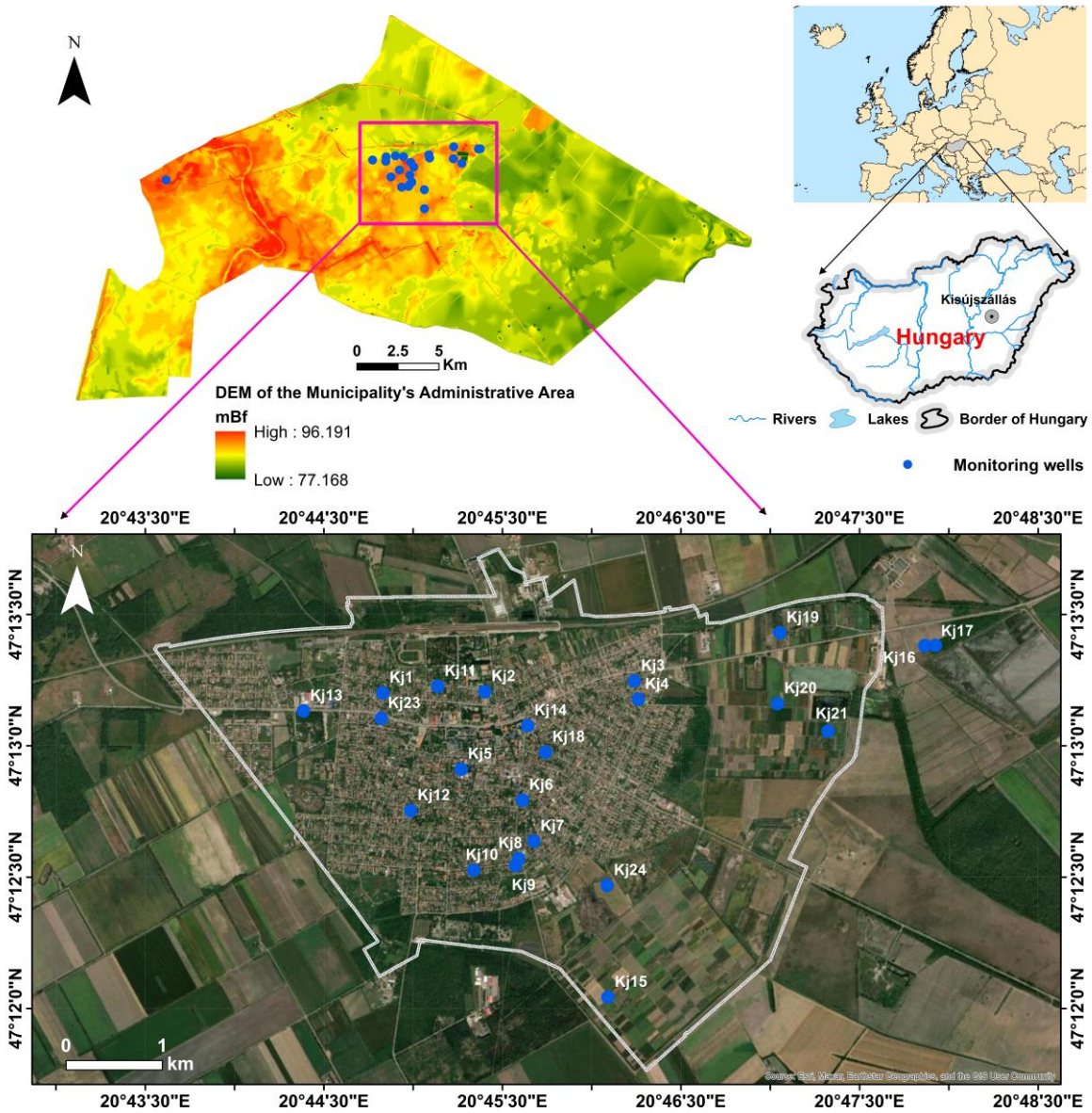


**Figure 1.** Location of the study area and the monitoring wells.

The geological structure consists predominantly of Quaternary fluvial deposits, with an 8–10 m thick upper sequence of fine-grained Pleistocene sediments, mainly loess-like silt and clay, overlying older alluvial formations. The shallow geological sequence is characterized by considerable lithological heterogeneity, with alternating clay, heavy clay, and silt layers, as well as locally occurring sandy deposits. The dominant soil types include Chernozems, Meadow soils, and Solonetz soils, reflecting the combined influence of alluvial sedimentation, shallow groundwater, and historical salinization processes. Salt-

affected soils are particularly characteristic of the lowland landscape, while clay-rich and clay-loam textures are widespread [37].

The region has a moderately warm and dry continental climate, with a mean annual temperature of approximately 10.2–10.4 °C and annual precipitation generally ranging from 490 to 510 mm [35]. Precipitation during the growing season averages approximately 300 mm, while the annual potential evaporation demand frequently exceeds precipitation, favoring periodic soil moisture deficits and salt accumulation. Shallow groundwater generally occurs at depths of 2–4 m, although considerable local variations have been documented. Groundwater chemistry is often influenced by natural salinity, with sodium-dominated bicarbonate waters occurring alongside calcium–magnesium bicarbonate groundwater. The combination of shallow groundwater, fine-grained sediments, salt-affected soils, and intensive agricultural land use creates a hydrogeologically sensitive environment in which both natural and anthropogenic processes may influence groundwater quality.

### *2.2. Groundwater Sampling, Field and Laboratory Measurements*

A total of 24 residential dug wells across the administrative area of Kisújszállás were surveyed in autumn 2026 (Figure 1), with the majority located within the urban residential area. Groundwater samples were collected from 22 wells, as two were dry at the time of sampling. Groundwater samples were collected in airtight, sealed sampling bottles and transported to the laboratory under refrigerated conditions, where the chemical analyses were performed within 24 h of sample collection.

The present study primarily focused on groundwater quality within the built-up residential area, while a limited number of wells from enclosed-garden and surrounding agricultural areas were included for exploratory purposes. Consequently, comparisons among land-use categories are preliminary. Based on the findings of this initial investigation, additional wells will be selected in future sampling campaigns to improve the representation of different land-use categories and allow a more detailed assessment of their hydrochemical differences.

At each sampling location, groundwater depth was measured relative to the well reference point. The elevations of the wells above mean sea level were determined using an Emlid Reach RX real-time kinematic (RTK) GNSS receiver (Emlid Tech Korlátolt Felelősségű Társaság, Budapest, Hungary), providing centimeter-level positioning precision. These measurements enabled the calculation of absolute groundwater elevations and the assessment of spatial variations in groundwater level. In situ physicochemical measurements included pH, electrical conductivity (EC), total dissolved solids (TDS), dissolved oxygen concentration (DO; mg/L), dissolved oxygen saturation (DO; %), oxidation–reduction potential (ORP), water temperature, salinity (PSU), and turbidity (FNU) using an HI7698594 portable multiparameter meter (Hanna Instruments).

Groundwater samples were collected for subsequent laboratory analysis at the Institute of Earth Sciences, University of Debrecen, Hungary. The investigated parameters, including ammonium ($NH_4^+$), nitrite ($NO_2^-$), nitrate ($NO_3^-$), phosphate ($PO_4^{3-}$), and chemical oxygen demand (COD), were determined according to Hungarian standards (HS ISO 7150-1:1992, HS 448-18:2009, HS 1484-13:2009, and HS 448-20:1990) [38–41]. Bicarbonate ($HCO_3^-$) and chloride ($Cl^-$) concentrations were determined according to Hungarian standards HS 448-11:1986 and HS 1484-15:2009, respectively [42,43]. Spectrophotometric analyses were performed using a SCHOTT Uvi Light UV–Vis spectrophotometer (SCHOTT Instruments, Mainz, Germany), with a manufacturer-specified photometric accuracy of ±0.005 absorbance units and a wavelength accuracy of ±1 nm.

The combined field and laboratory measurements provided the hydrochemical dataset used to evaluate groundwater quality, spatial contamination patterns, and relationships among the investigated parameters. The $NO_3^-/Cl^-$ molar ratios were calculated from the measured concentrations after conversion from mg/L to mmol/L using the respective molar masses. The pH and dissolved oxygen (DO) ranges associated with nitrification and denitrification 5 were defined based on previous studies [44,45].

The measured groundwater quality parameters were evaluated against the relevant contamination threshold values established by Hungarian Decree No. 6/2009 (IV. 14.) KvVM–EüM–FVM. The nitrate threshold of 50 mg/L is also consistent with the EU groundwater quality standard established by Directive 2006/118/EC, as amended.

### *2.3. Statistical and Geospatial Data Analysis*

Statistical analyses and graphical visualizations were performed using OriginPro 2025b (OriginLab Corporation, Northampton, MA, USA), while scatter plots were additionally prepared using Grapher 19 software (Golden Software, LLC, Golden, CO, USA). Geospatial analyses and cartographic representations were conducted using ArcGIS 10.4 (Esri, Redlands, CA, USA). Descriptive statistics were calculated to characterize the distribution and variability of the investigated groundwater quality parameters. Boxplots were used to illustrate differences in hydrochemical characteristics among sampling locations and subsequently identified groundwater groups. Spearman's rank correlation analysis was applied to assess relationships among physicochemical parameters, with statistical significance evaluated at $p < 0.05$.

Multivariate statistical techniques, including principal component analysis (PCA) and hierarchical cluster analysis (HCA), were employed to identify hydrochemical patterns and classify groundwater samples according to their physicochemical characteristics. Given the sample size ($n$ = 22), the statistical analyses were primarily applied as exploratory tools to identify hydrochemical relationships and patterns within the study area.

Prior to multivariate analysis, the variables were standardized using Z-score transformation to eliminate differences arising from measurement units and numerical scales. PCA was performed to reduce data dimensionality and identify the main gradients of hydrochemical variability, with the first two principal components visualized using a biplot. The same nine standardized hydrochemical parameters were used for both PCA and HCA to ensure consistency between the multivariate analyses: pH, EC, $HCO_3^-$, $NH_4^+$, $NO_2^-$, $NO_3^-$, $PO_4^{3-}$, $Cl^-$, and COD. TDS and salinity (PSU) were excluded because they largely reflect the same overall dissolved-ion content as EC. HCA was conducted using Ward's linkage method and Euclidean distance, and the resulting dendrogram was used to distinguish three groundwater groups. Differences among the identified clusters were subsequently evaluated using comparative boxplots and spatial representations.

The spatial distributions of groundwater elevations and selected hydrochemical parameters were evaluated in ArcGIS 10.4 using inverse distance weighting (IDW). IDW is a deterministic interpolation method that estimates values at unsampled locations as a weighted average of neighboring observations, assigning higher weights to geographically closer sampling points. The interpolated value was calculated as follows:

$$\hat{Z}(x_0) = \frac{\sum_{i=1}^{n} \frac{Z(x_i)}{d(x_0, x_i)^p}}{\sum_{i=1}^{n} \frac{1}{d(x_0, x_i)^p}}$$

where $\hat{Z}(x_0)$ is the interpolated value at an unsampled location; $Z(x_i)$ is the measured value at sampling point i; $d(x_0,x_i)$ is the distance between the prediction location and sampling point i; n is the number of neighboring sampling points; and p is the distance-weighting

exponent. Larger values of $p$ increase the relative influence of nearby observations [46]. To improve the spatial consistency of the interpolation, the most isolated sampling well (Kj22) was excluded from the IDW analysis, resulting in a dataset of 21 wells. The interpolation was performed using a distance-weighting exponent of $p = 2$ and the 12 nearest wells for each interpolated location. Leave-one-out cross-validation and sensitivity analysis were conducted using alternative distance-weighting exponents ($p = 1$ and $p = 3$) to assess interpolation performance and robustness. The resulting IDW maps represent spatial predictions of groundwater quality, estimating parameter values at unsampled locations based on the available measurements.

Groundwater elevations were calculated from surveyed well elevations and measured groundwater depths. Interpolated surfaces were used to visualize spatial variations across the study area, and the locations of hydrochemical clusters were compared with land-use categories. In addition, chloride concentration versus nitrate-to-chloride molar ratio scatter plots were used to support the interpretation of potential anthropogenic influences. Because sampling wells were unevenly distributed and concentrated mainly in the built-up area, interpolated patterns in sparsely sampled peripheral areas were interpreted cautiously.

## 3. Results

### *3.1. Spatial Distribution of Groundwater Levels*

The spatial distribution of surface elevations and groundwater levels is presented in Figure 2. The surveyed well reference elevations ranged from 84.51 to 87.56 m a.s.l., with a mean of 86.33 m a.s.l., reflecting the relatively uniform topography of the study area (Table 1). Groundwater depths varied considerably among the 24 investigated wells, ranging from 0.46 to 5.72 m, with a mean of 4.46 m and a median of 4.91 m. The calculated absolute groundwater elevations ranged from 80.14 to 84.57 m a.s.l., with a mean of 81.87 m a.s.l. (Table 1).

**Table 1.** Summary statistics of well reference elevations and groundwater levels.

| Parameter | Minimum | Maximum | Mean | Median |
|---|---|---|---|---|
| Well reference elevation (m a.s.l.) | 84.51 | 87.56 | 86.33 | 86.41 |
| Depth to groundwater (m) | 0.46 | 5.72 | 4.46 | 4.91 |
| Groundwater elevation (m a.s.l.) | 80.14 | 84.57 | 81.87 | 81.66 |

The interpolated groundwater-level map revealed pronounced spatial differences across the study area (Figure 2). Within the central built-up area, groundwater elevations generally ranged between 81.5 and 83.0 m a.s.l., with localized maxima exceeding 84.0 m a.s.l. in the northern and northeastern sections. In contrast, the southern part of the settlement was characterized by relatively lower groundwater elevations, predominantly between 80.5 and 82.0 m a.s.l. The eastern areas exhibited greater spatial variability, with localized groundwater-level maxima surrounded by zones of lower hydraulic head. A general decrease in groundwater elevations was observed from the northern part of the settlement towards the southern and southeastern areas, although local deviations from this spatial trend were found as well.

Despite the limited variation in surveyed well reference elevations (3.05 m), absolute groundwater levels exhibited a wider range of 4.43 m. Furthermore, the weak correlation between reference elevations and absolute groundwater levels ($r = 0.10$) indicates that groundwater elevations were not strongly associated with local topographic variations. The observed spatial heterogeneity suggests that groundwater-level distribution is influenced by additional local factors beyond surface topography. However, the available

measurements do not allow the relative contributions of groundwater recharge, subsurface hydraulic conditions, and potential anthropogenic water inputs to be determined.

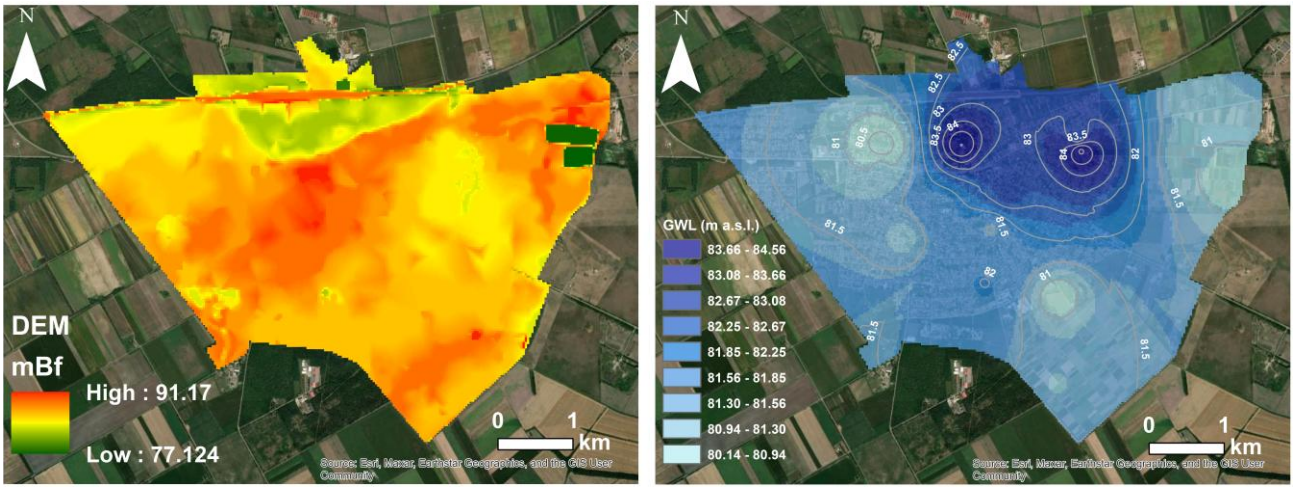


(**a**) (**b**)

**Figure 2.** Spatial distribution of surface elevation and groundwater levels in the study area: (**a**) digital elevation model (DEM); (**b**) interpolated groundwater elevations (m a.s.l.).

### *3.2. Descriptive Statistics of Groundwater Quality Parameters*

The descriptive statistics of the investigated groundwater quality parameters are presented in Table 2. Considerable variability was observed among the 22 groundwater samples, particularly in the parameters associated with salinity and nutrient enrichment.

**Table 2.** Descriptive statistics of the investigated physicochemical and hydrochemical parameters in shallow groundwater samples.

| Parameter | Unit | Limit | Skewness | Kurtosis | Mean | SD | Minimum | Q1 | Median | Q3 | Maximum | IQR |
|---|---|---|---|---|---|---|---|---|---|---|---|---|
| pH | | <6.5<br>9.0< | 1.563 | 2.555 | 7.603 | 0.411 | 7.04 | 7.37 | 7.495 | 7.75 | 8.79 | 0.38 |
| EC | µS/cm | 2500 | 1.27 | 1.309 | 2965.8 | 2122.75 | 367 | 1582 | 2500 | 4310 | 8460 | 2728 |
| TDS | mg/L | | 1.33 | 1.37 | 1521.9 | 1153.46 | 168 | 757 | 1266 | 2217 | 4504 | 1460 |
| $HCO_3^-$ | mg/L | | 1.461 | 4.173 | 18.397 | 7.865 | 4.762 | 14.285 | 17.618 | 20.474 | 43.33 | 6.19 |
| $NH_4^+$ | mg/L | 0.5 | 4.656 | 21.772 | 3.675 | 12.55 | 0.061 | 0.608 | 0.8 | 1.195 | 59.738 | 0.587 |
| $NO_2^-$ | mg/L | 0.5 | 3.112 | 8.882 | 0.147 | 0.356 | 0.011 | 0.018 | 0.028 | 0.054 | 1.395 | 0.036 |
| $NO_3^-$ | mg/L | 50 | 2.564 | 7.53 | 159.8 | 298.34 | 0.131 | 1.771 | 4.526 | 191.55 | 1233.28 | 189.7 |
| $PO_4^{3-}$ | mg/L | 0.5 | 2.546 | 7.25 | 1.129 | 1.407 | 0.158 | 0.286 | 0.645 | 1.069 | 6.132 | 0.783 |
| $Cl^-$ | mg/L | 250 | 3.251 | 11.783 | 302.8 | 493.59 | 22.728 | 50.001 | 134.092 | 300.00 | 2236.38 | 250.1 |
| COD | mg/L | | 0.729 | −0.182 | 9.339 | 4.779 | 1.499 | 6.499 | 8.165 | 11.082 | 19.414 | 4.583 |
| ORP | mV | | −0.628 | −0.473 | 11.88 | 145.92 | −269.1 | −70.2 | 25.95 | 135 | 205.1 | 205.2 |
| DO | % | | 1.248 | 2.521 | 52.92 | 20.044 | 20.4 | 40.8 | 49.8 | 59.2 | 112.1 | 18.4 |
| DO | mg/L | | 1.341 | 3.313 | 5.16 | 1.916 | 2.01 | 4.01 | 4.90 | 5.92 | 11.1 | 1.91 |
| PSU | | | 1.421 | 1.632 | 1.626 | 1.305 | 0.16 | 0.77 | 1.315 | 2.38 | 5.07 | 1.61 |
| FNU | | | 2.034 | 3.598 | 4.672 | 7.204 | 0 | 0.1 | 1.14 | 6.7 | 24.9 | 6.6 |
| Temp | °C | | 1.054 | 0.607 | 16.19 | 2.144 | 13.41 | 14.66 | 15.73 | 17.62 | 21.38 | 2.96 |

Groundwater pH ranged from 7.04 to 8.79, with a mean of 7.60, indicating predominantly neutral to alkaline conditions. Electrical conductivity (EC) varied substantially between 367 and 8460 µS/cm, with a mean of 2965.86 µS/cm and a median of 2500 µS/cm. Similarly, total dissolved solids (TDS) ranged from 168 to 4504 mg/L, reflecting considerable differences in groundwater salinity. The positively skewed distributions of EC (1.27) and TDS (1.33) indicate the presence of several highly mineralized groundwater samples.

Among the investigated nitrogen compounds, nitrate ($NO_3^-$) exhibited particularly pronounced variability, ranging from 0.131 to 1233.28 mg/L. The mean concentration

(159.89 mg/L) was considerably higher than the median (4.53 mg/L), accompanied by substantial positive skewness (2.56), indicating that a limited number of highly contaminated wells strongly influenced the overall distribution. The maximum concentration exceeded the Hungarian groundwater contamination threshold of 50 mg/L by approximately 25 times. Ammonium ($NH_4^+$) concentrations ranged from 0.061 to 59.74 mg/L, with a mean of 3.68 mg/L and a median of 0.80 mg/L. Its exceptionally high skewness (4.66) and kurtosis (21.77) indicated a strongly asymmetric distribution dominated by isolated elevated values. Nitrite ($NO_2^-$) concentrations were generally lower, with a median of 0.028 mg/L, although the maximum reached 1.395 mg/L. Phosphate ($PO_4^{3-}$) concentrations varied between 0.158 and 6.132 mg/L, with a mean of 1.13 mg/L and a median of 0.645 mg/L. The median phosphate concentration exceeded the applied contamination threshold of 0.5 mg/L, indicating relatively widespread phosphorus enrichment among the investigated wells.

Chloride ($Cl^-$) concentrations ranged from 22.73 to 2236.39 mg/L, with a mean of 302.90 mg/L and a median of 134.09 mg/L. The pronounced positive skewness (3.25) suggests that elevated chloride concentrations were concentrated in a limited number of groundwater samples. The substantial variability in EC, TDS, and chloride reflects marked differences in groundwater salinity, potentially associated with both natural salinity and anthropogenic inputs. Bicarbonate concentrations ranged from 4.762 to 43.33, while chemical oxygen demand (COD) varied between 1.50 and 19.41 mg/L, with a mean of 9.34 mg/L.

The investigated groundwater samples also exhibited considerable variation in oxygen availability and redox conditions. Dissolved oxygen saturation ranged from 20.4% to 112.1%, with a mean of 52.92%, indicating differences in groundwater oxygenation. Oxidation–reduction potential (ORP) varied from −269.1 to +205.1 mV, with a mean of 11.89 mV, reflecting substantial heterogeneity in measured redox conditions. Turbidity ranged from 0 to 24.9 FNU, while water temperature varied between 13.41 and 21.38 °C, with a mean of 16.20 °C. These results demonstrate pronounced spatial heterogeneity in groundwater quality, particularly in nitrate-, ammonium-, chloride-, and salinity-related parameters, providing a basis for subsequent spatial and multivariate analyses.

### *3.3. Correlations Among Hydrochemical Parameters*

Spearman's rank correlation analysis revealed several significant relationships among the investigated groundwater quality parameters (Figure 3). The strongest positive correlations were observed among electrical conductivity (EC), total dissolved solids (TDS), salinity (PSU), and chloride ($Cl^-$), indicating a closely associated group of salinity-related parameters. Bicarbonate ($HCO_3^-$) also exhibited significant positive correlations with EC, TDS, chloride, and PSU, although these relationships were comparatively weaker. In contrast, nitrate ($NO_3^-$) showed no statistically significant correlation with EC or chloride, suggesting that nitrate enrichment did not consistently coincide with increased groundwater salinity.

Significant negative correlations were identified between nitrate and pH, ammonium ($NH_4^+$), phosphate ($PO_4^{3-}$), and turbidity (FNU) (Figure 3). In contrast, nitrate exhibited a statistically significant positive correlation with oxidation–reduction potential (ORP) and was also positively correlated with dissolved oxygen saturation (DO%), indicating a tendency towards higher nitrate concentrations under more oxygenated conditions. Ammonium exhibited significant negative correlations with nitrate, ORP, and DO%, while positive correlations were observed with phosphate and turbidity. Phosphate was also positively associated with COD and negatively correlated with nitrate. These relationships reveal contrasting hydrochemical patterns among nitrogen species and suggest that nutrient concentrations are associated with differences in groundwater oxygenation and

redox conditions. Nevertheless, the observed correlations represent statistical associations and do not independently establish the underlying biogeochemical processes.

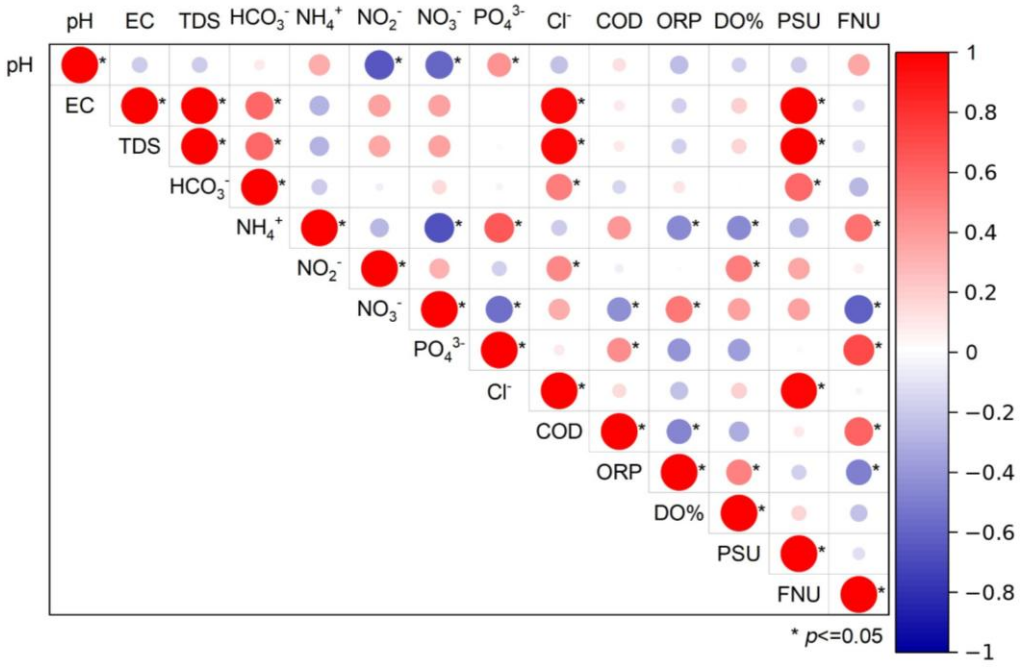


**Figure 3.** Spearman's rank correlation matrix of the investigated groundwater quality parameters. Circle size and color indicate the strength and direction of the correlations; asterisks denote statistically significant relationships ($p < 0.05$).

The relationships among DO, ORP, $NO_3^-$, and $NH_4^+$ were further examined using a scatterplot matrix (Figure 4). DO concentrations exhibited considerable variability, with most measurements ranging between approximately 3 and 6 mg/L, while ORP values extended from −269.1 to +205.1 mV. The DO–ORP scatterplot indicated a generally positive association, although substantial dispersion was observed, particularly at intermediate oxygen concentrations.

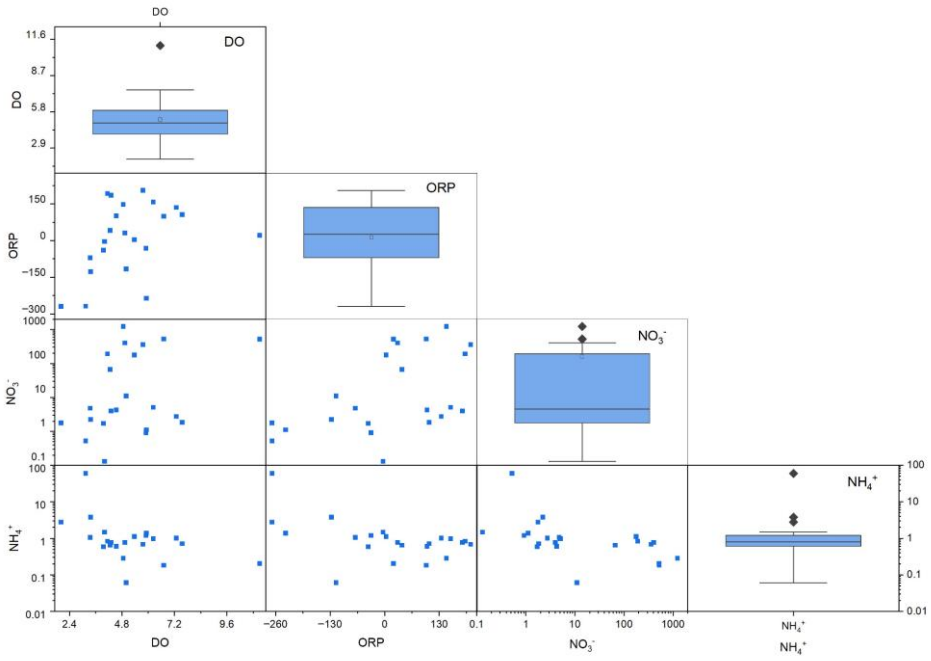

**Figure 4.** Scatterplot matrix illustrating the relationships among DO, ORP, $NO_3^-$, and $NH_4^+$ concentrations in groundwater samples.

$NO_3^-$ concentrations varied over several orders of magnitude, from 0.131 to 1233.28 mg/L, with the highest values generally occurring in samples characterized by moderate to elevated DO concentrations. However, $NO_3^-$ concentrations exhibited considerable variability at similar dissolved oxygen levels. Spearman correlation analysis revealed a statistically significant positive relationship between $NO_3^-$ and ORP, while ORP was also positively correlated with dissolved oxygen saturation (DO%).

In contrast, $NH_4^+$ concentrations were predominantly below 2 mg/L, with a small number of markedly elevated observations reaching 59.74 mg/L. Higher $NH_4^+$ concentrations tended to occur under relatively low-oxygen and negative-ORP conditions, although the relationships were not uniform. The contrasting distributions of $NO_3^-$ and $NH_4^+$ are consistent with spatially heterogeneous groundwater conditions, potentially involving differences in nitrogen inputs and redox-dependent transformations. The considerable scatter indicates that additional hydrochemical and environmental factors may influence the observed nitrogen concentrations.

The relationship between dissolved oxygen concentration (DO mg/L) and pH was examined to further characterize groundwater conditions associated with nitrogen transformations (Figure 5). Most groundwater samples exhibited pH values between 7.0 and 8.0, while DO concentrations generally ranged from 3 to 7 mg/L. Three wells (Kj2, Kj9, and Kj15) displayed distinctly alkaline conditions, with pH values exceeding 8.0. The highest DO concentration (approximately 11 mg/L) was recorded at Kj22, whereas the lowest values, around 2–3 mg/L, occurred at Kj9 and Kj15. These observations suggest that the predominantly neutral to moderately alkaline pH and relatively high dissolved oxygen concentrations provided conditions favorable for nitrification in most of the investigated groundwater samples.

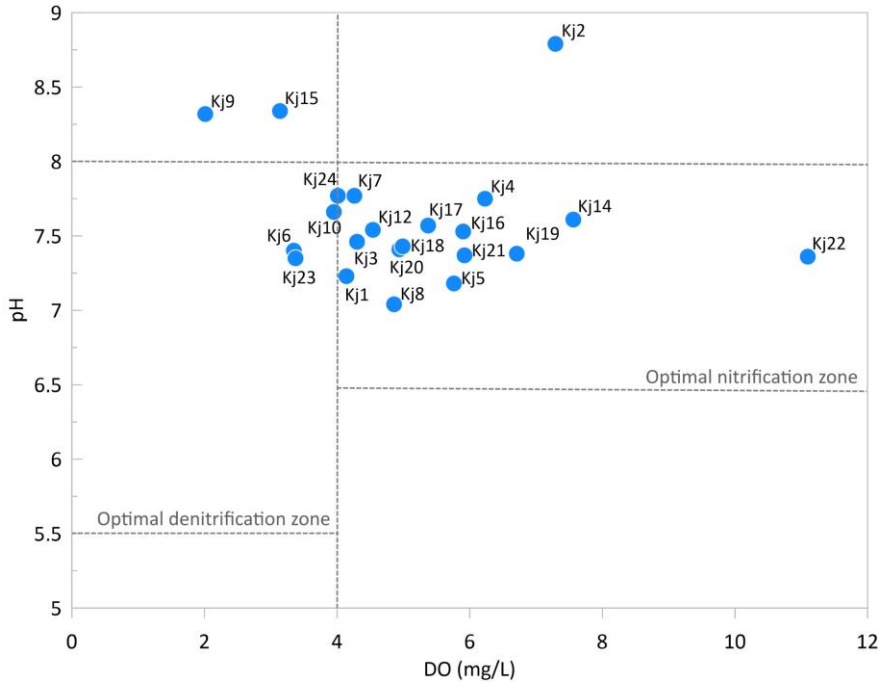


**Figure 5.** Relationship between dissolved oxygen (DO) concentration and pH in the investigated groundwater wells.

### *3.4. Spatial Distribution of Selected Hydrochemical Parameters*

The spatial distribution of EC, $Cl^-$, $NO_3^-$, and $PO_4^{3-}$ revealed considerable heterogeneity in shallow groundwater quality across the study area (Figure 6). EC ranged from 384 to 8452 µS/cm, while $Cl^-$ concentrations varied between 23 and 2233 mg/L. Both parameters exhibited similar spatial patterns, with pronounced maxima concentrated in the northeastern part of the settlement and relatively lower values in the western and northwestern sectors. The spatial correspondence between EC and $Cl^-$ indicates that elevated groundwater salinity is closely associated with $Cl^-$ enrichment. Within the built-up area, this enrichment may be related to historical domestic wastewater infiltration, leakage from sewage infrastructure, and household activities, whereas natural salt accumulation in the surrounding saline soils may also contribute to elevated concentrations.

$NO_3^-$ exhibited a more heterogeneous spatial distribution, with concentrations ranging from 0.363 to 1230 mg/L (Figure 6). Distinct concentration maxima occurred in the northeastern and central-southern parts of the settlement, indicating localized zones of substantial $NO_3^-$ enrichment. Within residential areas, these hotspots may reflect historical sewage effluent infiltration from former cesspits, potential leakage from existing sewer networks, and nitrogen inputs associated with fertilizer application in household gardens. In peripheral areas, agricultural fertilizer application, manure management, and wastewater disposal from isolated residential properties may represent additional potential sources. The spatially separated $NO_3^-$ maxima suggest that contamination is influenced by multiple localized inputs rather than a single uniform pollution source.

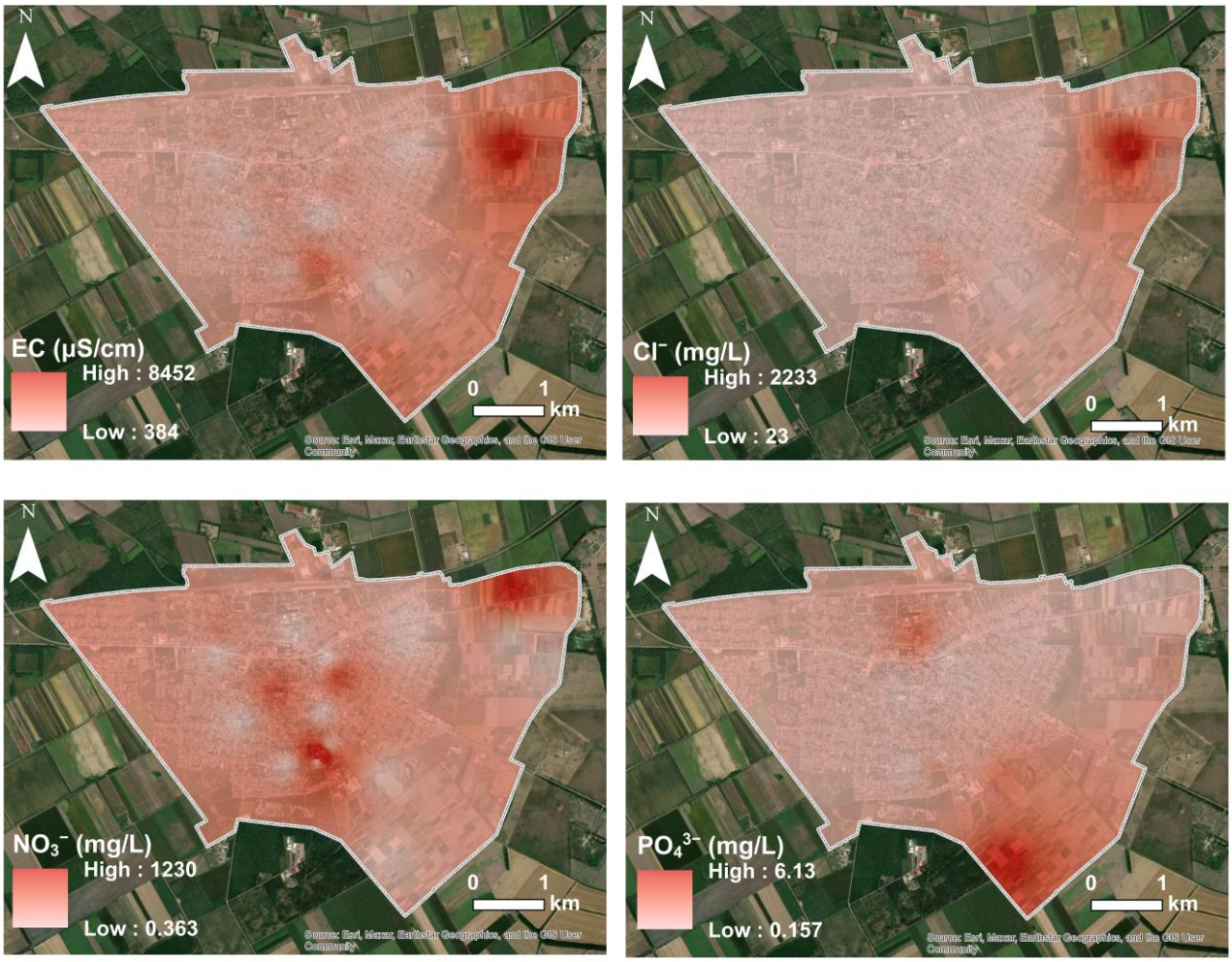


**Figure 6.** Spatial distribution of EC, $Cl^-$, $NO_3^-$, and $PO_4^{3-}$ in shallow groundwater within the inner administrative area of the study site, based on inverse distance weighting (IDW) interpolation.

$PO_4^{3-}$ concentrations ranged from 0.157 to 6.13 mg/L, with the highest values concentrated in the southern and southeastern parts of the study area (Figure 6). Additionally, less pronounced concentration maxima occurred in the central and northern sectors. Within the settlement, elevated $PO_4^{3-}$ concentrations may be associated with domestic wastewater and fertilizer use in residential gardens. In peripheral areas, agricultural activities, manure application, and wastewater infiltration from properties not connected to centralized sewerage may also contribute to phosphorus enrichment. The limited spatial overlap between $PO_4^{3-}$ and the EC–$Cl^-$ maxima indicates that their distributions are influenced by partly different local conditions. The observed patterns are consistent with multiple potential anthropogenic influences, including domestic wastewater, household gardening, and agricultural activities, superimposed on the natural hydrogeochemical characteristics of the shallow aquifer.

### *3.5. Hydrochemical Classification of Groundwater Using HCA*

Hierarchical cluster analysis (HCA) identified three distinct groundwater groups based on their hydrochemical characteristics (Figure 7). Cluster 1 comprised 14 wells (63.6%), representing the largest and relatively more homogeneous group, whereas Cluster 2 included six wells (27.3%). Cluster 3 consisted of only two wells (9.1%; Kj8 and Kj22), which were clearly separated from the remaining sampling locations at a relatively high linkage distance. The dendrogram indicated the greatest dissimilarity between Cluster 1 and the other two groups, reflecting substantial differences in groundwater chemistry across the investigated wells.

The hydrochemical characteristics of the identified groups were further evaluated using cluster-specific boxplots (Figure 8). Cluster 1 was characterized by relatively lower salinity, with mean EC and $Cl^-$ concentrations of 1930 µS/cm and 106.17 mg/L, respectively. Nevertheless, considerable variability in $NO_3^-$ concentrations was observed, with a mean of 124.68 mg/L and a maximum of 524.80 mg/L, indicating that this group also included substantially nitrate-enriched groundwater samples. The median $NO_3^-$ concentration was considerably lower (4.95 mg/L), reflecting the influence of several highly contaminated wells on the group mean.

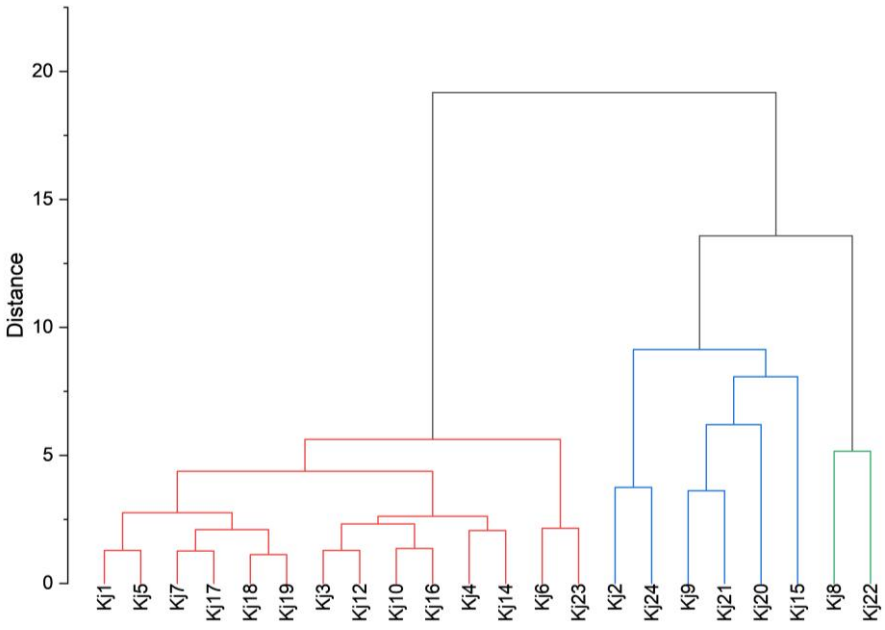


**Figure 7.** Hierarchical cluster analysis (HCA) dendrogram of the investigated groundwater samples based on standardized hydrochemical parameters using Ward's linkage method and Euclidean distance.

Cluster 2 exhibited elevated salinity and pronounced enrichment in $NH_4^+$ and $PO_4^{3-}$. Mean EC and $Cl^-$ concentrations reached 4174 µS/cm and 594.70 mg/L, respectively, while mean $NH_4^+$ and $PO_4^{3-}$ concentrations were 11.07 and 2.80 mg/L. In contrast, $NO_3^-$ concentrations remained comparatively low, with a mean of 2.89 mg/L (Figure 8). This group also exhibited the lowest mean ORP (−126.57 mV), suggesting predominantly more reducing hydrochemical conditions. The combination of elevated $NH_4^+$, $PO_4^{3-}$, and relatively low $NO_3^-$ concentrations distinguished Cluster 2 from the other groundwater groups.

Cluster 3 was characterized by the highest salinity and $NO_3^-$ enrichment, with mean EC and $NO_3^-$ values of 6590 µS/cm and 877.40 mg/L, respectively (Figure 8). Mean $Cl^-$ concentrations reached 804.55 mg/L, while ORP averaged +84.25 mV. In contrast to Cluster 2, $NH_4^+$ and $PO_4^{3-}$ concentrations remained relatively low, averaging 0.24 and 0.33 mg/L, respectively. These characteristics indicate a distinct hydrochemical signature associated with substantial nitrate enrichment under comparatively more oxidizing conditions. However, given the limited number of wells in Cluster 3 ($n$ = 2), its descriptive statistics should be interpreted cautiously.

The HCA and cluster-specific distributions revealed three different hydrochemical patterns: a heterogeneous group with generally lower salinity (Cluster 1), a more mineralized group characterized by $NH_4^+$ and $PO_4^{3-}$ enrichment and lower ORP (Cluster 2), and a highly mineralized, nitrate-enriched group (Cluster 3). These differences demonstrate the substantial hydrochemical heterogeneity of shallow groundwater within the investigated settlement.

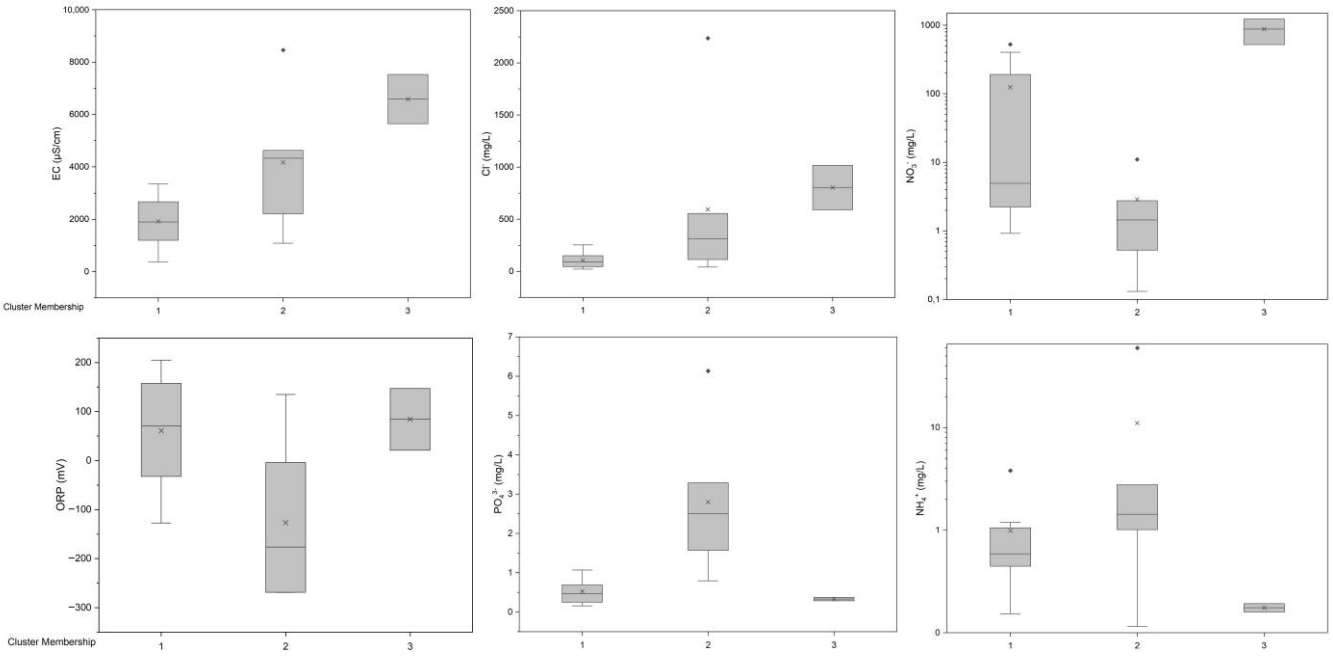


**Figure 8.** Boxplots illustrating the distributions of EC, $Cl^-$, $NO_3^-$, ORP, $PO_4^{3-}$, and $NH_4^+$ across the three groundwater clusters identified by HCA. Crosses indicate mean values, while diamonds represent outliers. The spatial distribution of the HCA-derived groundwater clusters suggests a possible relationship with land-use categories (Figure 9). Cluster 1 predominates in the inner administrative area, indicating that this group represents the most typical hydrochemical conditions of the built-up part of the settlement. At the same time, several Cluster 1 wells are also located near the eastern and northeastern margins of the study area, suggesting that this hydrochemical type is not restricted exclusively to the residential core. Cluster 2 is more frequently associated with peripheral parts of the study area and is notably represented in the enclosed garden areas, particularly in the southeastern and northeastern sectors. However, some Cluster 2 wells also occur within the inner administrative area, indicating transitional hydrochemical characteristics. Cluster 3 consists of two

spatially separated wells: one located in the inner administrative area (Kj8) and another in the outer administrative area at the western margin of the municipality (Kj22). This pattern suggests that the most distinctive hydrochemical conditions are influenced by local factors. To better characterize hydrochemical differences among land-use categories, future investigations will include additional wells in land-use categories that are currently underrepresented in the sampling network.

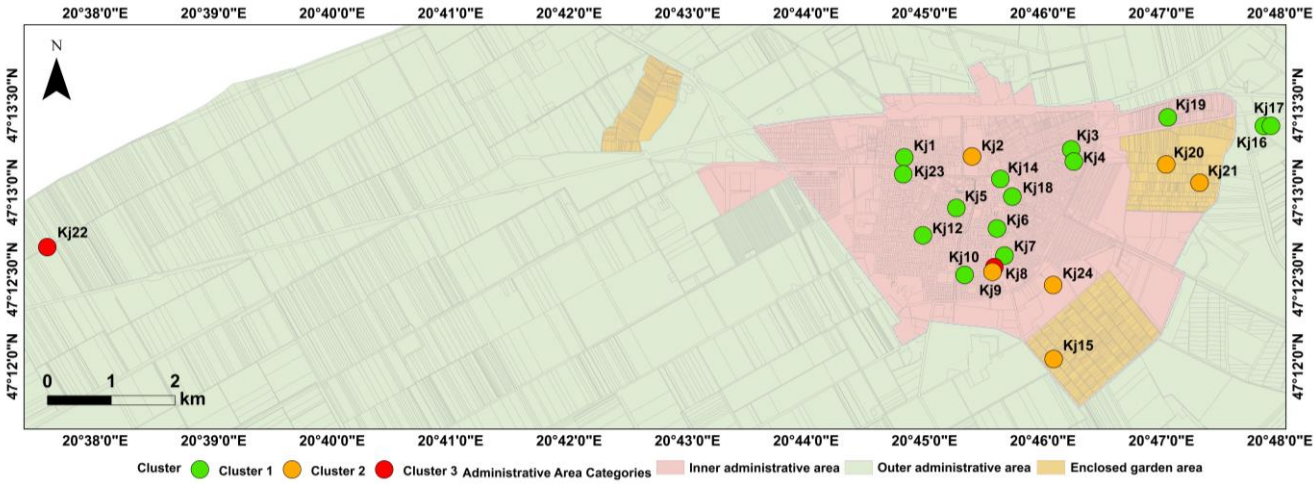


**Figure 9.** Spatial distribution of the HCA-derived groundwater clusters in relation to the inner administrative area, enclosed garden area, and outer administrative area of the study area.

### *3.6. Principal Component Analysis of Groundwater Hydrochemistry*

Principal component analysis (PCA) was performed using nine standardized hydrochemical parameters to identify the principal patterns of groundwater quality variability and examine their relationships with the HCA-derived clusters (Figure 10). The first three principal components had eigenvalues greater than 1 and collectively explained 82.38% of the total variance. PC1 accounted for 36.48%, PC2 for 31.05%, and PC3 for 14.84%, while the first two components together explained 67.54% of the total variability.

PC1 was primarily associated with positive contributions from $NO_2^-$ (0.465), $NO_3^-$ (0.439), EC (0.343), and $Cl^-$ (0.268), whereas pH (−0.349) and $PO_4^{3-}$ (−0.313) showed negative coefficients. This component therefore represents a hydrochemical gradient contrasting oxidized nitrogen enrichment and groundwater salinity with relatively elevated pH and $PO_4^{3-}$ concentrations. PC2 was characterized by positive coefficients for $PO_4^{3-}$ (0.439), $NH_4^+$ (0.437), EC (0.410), $HCO_3^-$ (0.380), and COD (0.322), suggesting that nutrient enrichment, dissolved constituents, and organic matter-related characteristics jointly contributed to this axis.

The PCA biplot revealed a clear correspondence between the principal component scores and the HCA-derived groundwater clusters (Figure 10). Cluster 1 samples were concentrated near the origin and predominantly occupied the negative PC2 region, indicating comparatively moderate hydrochemical characteristics. Cluster 2 displayed greater dispersion, particularly along PC2, with Kj15 clearly separated in the upper-left quadrant, reflecting its distinct hydrochemical composition. Other Cluster 2 samples, including Kj9 and Kj12, were associated with the negative PC1 direction, where $NH_4^+$, $PO_4^{3-}$, COD, and pH exhibited stronger contributions. In contrast, Cluster 3 wells (Kj8 and Kj22) occupied distinctly positive PC1 positions, closely aligned with the $NO_3^-$ and $NO_2^-$ vectors. Their separation confirms the substantial contribution of oxidized nitrogen compounds to the distinctive hydrochemical characteristics of this group.

PC3 explained an additional 14.84% of the total variance and was primarily characterized by negative coefficients for $Cl^-$ (−0.562) and COD (−0.467), and a positive coefficient for $HCO_3^-$ (0.404). This component reflects additional hydrochemical variability,

contrasting chloride and COD enrichment with bicarbonate-related characteristics, and complements the patterns identified by PC1 and PC2.

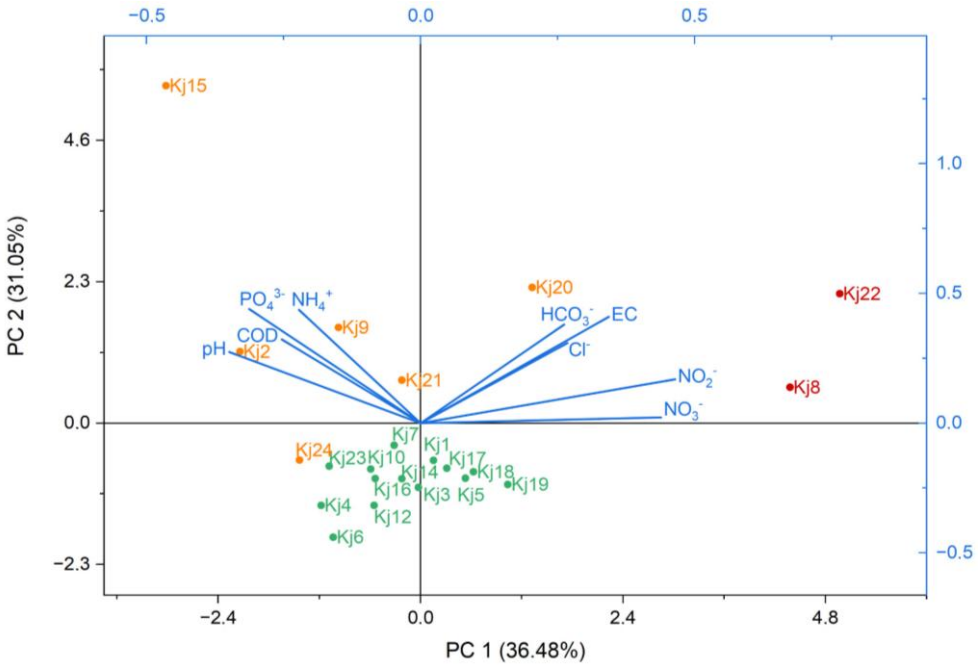


**Figure 10.** Principal component analysis (PCA) biplot of groundwater samples, with sampling locations classified according to the three HCA-derived clusters.

The results of PCA support the HCA classification and indicate that groundwater variability is primarily structured by two contrasting hydrochemical patterns: oxidized nitrogen enrichment associated with increased salinity, and elevated $NH_4^+$, $PO_4^{3-}$, and organic matter-related parameters. The distribution of the groundwater clusters along these gradients highlights the heterogeneous hydrochemical conditions across the investigated settlement.

### *3.7. Potential Sources of Groundwater Contamination*

The relationship between $Cl^-$ concentrations and $NO_3^-/Cl^-$ molar ratios was examined to assess potential differences in anthropogenic contamination sources among the HCA-derived groundwater clusters (Figure 11). The investigated samples exhibited substantial variability in both parameters, with $Cl^-$ concentrations extending over more than two orders of magnitude and $NO_3^-/Cl^-$ ratios ranging from approximately 0.001 to 2.0. The distribution of the samples revealed contrasting hydrochemical characteristics among the three clusters. Although elevated chloride concentrations may partly result from natural salinization, the markedly elevated nitrate concentrations observed in several wells clearly indicate anthropogenic contamination. Therefore, the $NO_3^-/Cl^-$ molar ratio provides useful information on relative nitrate enrichment, although it cannot independently distinguish between agricultural and domestic wastewater sources. Further isotopic analyses will be necessary to identify the specific sources of nitrate contamination.

Cluster 1 exhibited considerable variability in $NO_3^-/Cl^-$ ratios (approximately 0.02–1.7), with several wells (Kj5, Kj18, and Kj19) showing pronounced nitrate enrichment relative to chloride. These characteristics may reflect fertilizer application in household gardens, agricultural nitrogen inputs, and historical domestic wastewater infiltration.

Cluster 2 was characterized by consistently low $NO_3^-/Cl^-$ ratios, predominantly below 0.01, combined with relatively elevated $Cl^-$ concentrations. This pattern is consistent

with potential domestic wastewater and manure-related inputs, although nitrate attenuation under reducing conditions may also contribute to the low ratios. This interpretation is supported by the elevated $NH_4^+$ and $PO_4^{3-}$ concentrations and predominantly negative ORP values observed in this cluster.

In contrast, Cluster 3 exhibited elevated $Cl^-$ concentrations accompanied by substantially higher $NO_3^-/Cl^-$ ratios, indicating pronounced nitrate enrichment and potentially overlapping anthropogenic influences. Although Cluster 3 contains only two wells (Kj8 and Kj22), their marked separation in both the HCA and PCA demonstrates a distinct hydrochemical pattern, particularly characterized by pronounced nitrate enrichment. These findings provide an important basis for future investigations, including the selection of additional sampling wells in currently underrepresented land-use categories, to better characterize the spatial distribution and extent of the identified hydrochemical patterns.

The observed hydrochemical patterns suggest that groundwater quality is affected by multiple potential contamination sources, including domestic wastewater, household gardening, and agricultural activities. However, natural salt accumulation in the region's saline soils may also contribute to elevated $Cl^-$ concentrations, highlighting the need for cautious source attribution based on ionic ratios alone.

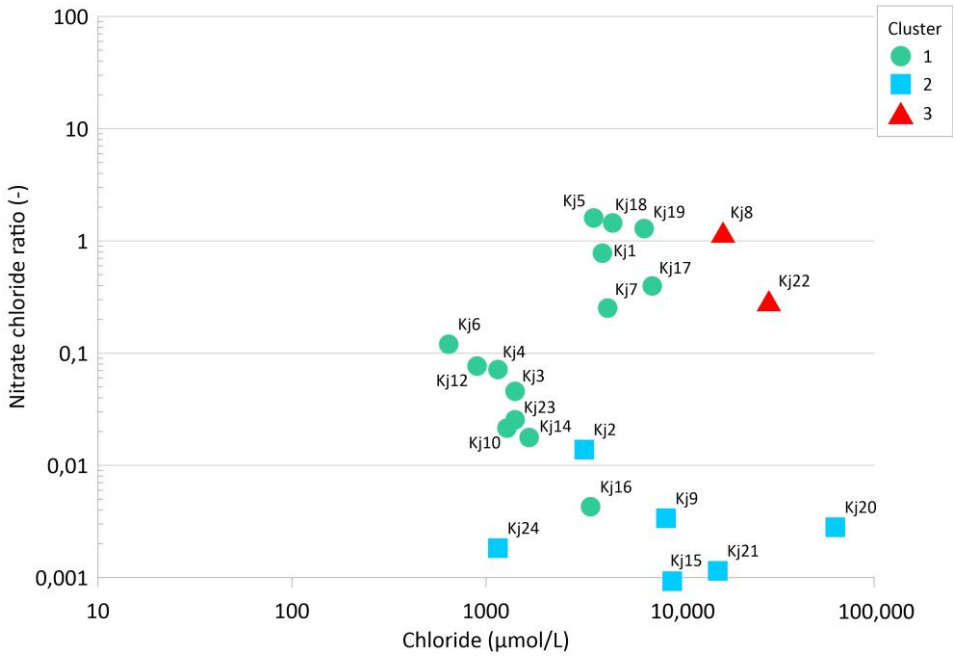


**Figure 11.** Relationship between $Cl^-$ concentrations and $NO_3^-/Cl^-$ molar ratios in shallow groundwater samples, classified according to the three HCA-derived clusters.

## 4. Discussion

The pronounced spatial variability in groundwater quality observed in the study area is consistent with findings from European and international studies demonstrating the combined influence of domestic wastewater and agricultural activities on shallow aquifers. In Sardinia, Italy, Biddau et al. investigated 60 groundwater samples and reported $NO_3^-$ concentrations ranging from 1 to 165 mg/L [47]. Their integrated hydrochemical and isotopic analyses identified manure as a predominant nitrate source, with additional contributions from domestic sewage and agricultural activities. Similar contamination patterns were documented by Aleku et al. in the eastern Niger Delta, Nigeria, where shallow groundwater quality was affected by municipal wastewater and inadequate sanitation infrastructure [48]. More recently, Riedel et al. investigated urban groundwater quality in a

medium-sized European city using monitoring data from 64 wells collected over more than 15 years. Their results revealed the widespread occurrence of anthropogenic contaminants, with an average of 14 emerging substances detected per well [10]. Furthermore, Wei et al., investigating groundwater nitrate sources in China, estimated contributions of 36.3% from chemical fertilizers and 35.4% from sewage and manure [49]. Compared with these studies, several wells in the study area exhibited considerably higher $NO_3^-$ concentrations, reaching a maximum of 1233.28 mg/L. The elevated nitrate concentrations observed at multiple sampling locations suggest the influence of local anthropogenic contamination inputs, potentially associated with historical domestic wastewater infiltration, household gardening, and agricultural activities. Further targeted investigations, including additional sampling wells, seasonal monitoring, and isotopic analyses, will be necessary to better characterize the spatial distribution of nitrate contamination and identify its specific sources.

The contrasting hydrochemical characteristics of the HCA-derived clusters highlight the potential role of redox-dependent nitrogen transformations in shallow groundwater. Cluster 2 exhibited elevated $NH_4^+$ and $PO_4^{3-}$ concentrations, low $NO_3^-$ levels, and predominantly negative ORP values, whereas Cluster 3 was characterized by pronounced $NO_3^-$ enrichment under comparatively more oxidizing conditions. Given the relatively small dataset, multivariate patterns may be sensitive to variable selection and extreme samples. Similar hydrochemical processes were investigated by Martinelli et al. in the Po Plain, Northern Italy, using a comprehensive database of nitrate and boron isotopes [50]. Their results revealed isotopic evidence of denitrification in approximately 22% of the investigated groundwater data, with nitrate reductions reaching 70–80% of the original concentrations in affected groundwater. The study also identified manure, synthetic fertilizers, and domestic sewage as important anthropogenic nitrogen sources. These findings support the interpretation that the contrasting nitrogen distributions observed in the study area may reflect differences in both contamination sources and subsurface biogeochemical conditions. The predominantly neutral to moderately alkaline pH and measurable DO concentrations further suggest that conditions favorable for nitrification prevail in several wells. Nevertheless, the occurrence and intensity of individual nitrogen transformation processes cannot be confirmed without additional isotopic or microbiological investigations.

Elevated groundwater salinity represents another important characteristic of the study area. The strong relationship between EC and $Cl^-$, together with the localized salinity hotspots, suggests that groundwater salinity may reflect both anthropogenic inputs and natural hydrogeochemical processes. Katz et al., investigating groundwater from major aquifers in the United States, demonstrated that chloride-based indicators, particularly Cl/Br ratios, can help identify potential impacts from septic systems when combined with land-use and hydrogeological information [29]. However, natural salinization must also be considered in the Great Hungarian Plain, where shallow groundwater and salt-affected soils are closely related. Tóth et al. demonstrated that groundwater elevation, dominant ionic composition, and subsurface texture were important factors influencing the spatial distribution of saline and sodic soils in the region [51]. Similarly, Bakacsi et al. (2019) highlighted the importance of groundwater depth and irrigation practices in assessing soil salinization and structural degradation risks in Hungary [52]. Accordingly, the elevated EC and $Cl^-$ concentrations observed in the study area cannot be attributed exclusively to wastewater contamination. Although natural salinization may contribute to elevated $Cl^-$ concentrations, the high $NO_3^-$ concentrations observed in several wells clearly indicate anthropogenic contamination. The $NO_3^-/Cl^-$ molar ratios therefore provide useful information on differences in nitrate enrichment, while further isotopic investigations are needed to distinguish the specific contamination sources.

The combined application of HCA, PCA, and spatial analysis provided further insight into the hydrochemical heterogeneity of shallow groundwater. Gulgundi and Shetty, investigating 67 groundwater sampling locations in Bengaluru, India, identified two distinct groundwater groups and demonstrated that Mg, $Cl^-$, and $NO_3^-$ were the main parameters differentiating spatial water-quality patterns [53]. In the present study, HCA distinguished three hydrochemical groups characterized by differences in salinity, nutrient concentrations, and redox conditions. PCA further supported these distinctions, with the first three principal components explaining 82.38% of the total variance. The spatial distribution of the clusters suggested a possible association with land-use categories, suggesting that residential areas, enclosed gardens, and agricultural surroundings may be affected by different combinations of anthropogenic and natural influences. Similarly, Mohammed et al. (2025) applied principal component analysis (PCA) to identify the main factors controlling groundwater hydrochemical variability in the Quaternary aquifer system of Debrecen, Hungary [54].

While the present study focuses on identifying spatial hydrochemical patterns, previous studies have demonstrated that the assessment of contaminant migration requires consideration of temporal changes and subsurface transport processes. Recent approaches combining spatiotemporal clustering with predictive modelling [55] and analytical solutions of advection–dispersion equations [56] provide complementary frameworks for investigating these processes.

Although the number of wells differed among land-use categories, the sampling network was primarily designed to characterize groundwater conditions within the built-up area, with additional wells providing exploratory information from surrounding areas. The two wells forming Cluster 3 represent a distinct hydrochemical pattern characterized by pronounced nitrate enrichment. Overall, the study demonstrates considerable local hydrochemical heterogeneity and highlights the combined influence of anthropogenic inputs and natural salinization on groundwater quality.

Study limitations: The present investigation provides a detailed assessment of shallow groundwater quality based on 22 samples collected during a single campaign in autumn 2026. As the sampling primarily focused on the built-up area, the representation of surrounding land-use categories was more limited. Future investigations will therefore include additional wells in underrepresented land-use categories and seasonal sampling to better characterize spatial and temporal differences in groundwater quality. Although the spatial and multivariate analyses revealed distinct hydrochemical patterns, the interpretation of these results should consider the limited number of samples in certain groups, particularly Cluster 3. Furthermore, additional isotopic investigations will be necessary to more precisely identify nitrate contamination sources and better understand the processes influencing groundwater chemistry.

## 5. Conclusions

This study provides an integrated assessment of shallow groundwater quality in Kisújszállás, Hungary, revealing substantial spatial and hydrochemical heterogeneity within an urban–agricultural environment. The investigation of 24 dug wells, including 22 with complete hydrochemical datasets, identified considerable differences in groundwater levels, salinity, nutrient concentrations, and redox conditions. Groundwater elevations ranged from 80.14 to 84.57 m a.s.l., while maximum $NO_3^-$ and $Cl^-$ concentrations reached 1233.28 and 2236.39 mg/L, respectively, substantially exceeding the relevant contamination thresholds.

Multivariate statistical analyses identified three distinct hydrochemical groups. Cluster 1 exhibited generally lower salinity but variable $NO_3^-$ enrichment, whereas Cluster 2 was characterized by elevated $NH_4^+$ and $PO_4^{3-}$ concentrations and predominantly

reducing conditions. Cluster 3 showed pronounced $NO_3^-$ contamination and high salinity. PCA supported these differences, with the first three principal components explaining 82.38% of the total variance. The spatial distribution of the clusters suggested a possible association with land-use categories.

The combined evaluation of hydrochemical parameters, redox conditions, and $NO_3^-/Cl^-$ molar ratios suggests that groundwater contamination reflects overlapping anthropogenic influences, including historical domestic wastewater infiltration, household gardening, and agricultural activities, while natural salinization may also contribute to elevated salinity. These findings highlight the complex nature of groundwater contamination in lowland settlements and demonstrate the importance of integrated monitoring approaches for identifying areas with elevated concentrations and supporting groundwater protection. Further seasonal monitoring and isotopic investigations are recommended to improve contamination source identification and understanding of nitrogen transformation processes.

**Author Contributions:** Conceptualization, T.M., M.V., T.K. and D.B.; methodology, T.M., M.V., T.K. and D.B.; software, T.M. and D.B.; validation, T.M., M.V. and T.K.; formal analysis, T.M.; investigation, T.M., M.V. and T.K.; resources, T.M. M.V. and T.K.; data curation, T.M., M.V. and T.K.; writing—original draft preparation, T.M. M.V. and T.K.; writing—review and editing, T.M. M.V. and T.K.; visualization, T.M. and D.B.; supervision, T.M., M.V. and T.K. All authors have read and agreed to the published version of the manuscript.

**Funding:** Supported by the University of Debrecen Program for Scientific Publication.

**Institutional Review Board Statement:** Not applicable.

**Informed Consent Statement:** Not applicable.

**Data Availability Statement:** The data presented in this study are available upon request from the corresponding author.

**Acknowledgments:** The authors acknowledge the support provided by the Municipality of Kisújszállás during the research.

**Conflicts of Interest:** The authors declare no conflicts of interest.

## References

1. Mbae, M.; Hansen, P.; Way, C.; Mills, F.; Willetts, J.; Foster, T.; Evans, B. Onsite Sanitation Systems and Contamination of Groundwater: A Systematic Review of the Evidence for Risk Using the Source-Pathway-Receptor Model. *PLoS Water* **2024**, *3*, e0000167. https://doi.org/10.1371/journal.pwat.0000167.
2. Janža, M.; Prestor, J.; Pestotnik, S.; Jamnik, B. Nitrogen Mass Balance and Pressure Impact Model Applied to an Urban Aquifer. *Water* **2020**, *12*, 1171. https://doi.org/10.3390/w12041171.
3. Hannan, M.; Lu, C.; Waqas, M.; Khan, A.U.; Liu, B. Regional Heterogeneity in Groundwater Response Driven by Land-Use Transitions across Pakistan. *J. Hydrol. Reg. Stud.* **2025**, *62*, 102958. https://doi.org/10.1016/j.ejrh.2025.102958.
4. Wang, L.; Xiao, Y.; Zhao, Z.; Qin, G.; Hu, W.; Chen, H.; Yang, S.; Zhang, Y.; Wang, J.; Yang, H.; et al. Hydrogeochemical Heterogeneity, Driving Forces, and Human Health Risk of Groundwater in an Arid Alluvial Fan Plain on Tibetan Plateau. *Hum. Ecol. Risk Assess. Int. J.* **2025**, *31*, 412–433. https://doi.org/10.1080/10807039.2025.2477503.
5. Bousouis, A.; Bouabdli, A.; Ayach, M.; Lazar, H.; Ravung, L.; Valles, V.; Barbiero, L. Discrimination of Spatial and Temporal Variabilities in the Analysis of Groundwater Databases: Application to the Bourgogne-Franche-Comté Region, France. *Water* **2025**, *17*, 384. https://doi.org/10.3390/w17030384.
6. Khairunnisa, S.S.N.; Yanidar, R.; Marendra, S.M.P.; Astuti, A.D.; Taki, H.M. The Study of Septic Tank Proximity on Coliform, *E. coli*, and Organic Contamination in Shallow Groundwater: A Case Study of DKI Jakarta. *J. Community Based Environ. Eng. Manag.* **2025**, *9*, 53–62. https://doi.org/10.23969/jcbeem.v9i1.21644.

7. Kim, M.; Koh, E.-H.; Kim, J. Field Study and Numerical Modeling to Assess the Impact of On-Site Septic Systems on Groundwater Quality of Jeju Island, South Korea. *Hydrology* **2024**, *11*, 146. https://doi.org/10.3390/hydrology11090146.
8. Wakida, F.T.; Lerner, D.N. Non-Agricultural Sources of Groundwater Nitrate: A Review and Case Study. *Water Res.* **2005**, *39*, 3–16. https://doi.org/10.1016/j.watres.2004.07.026.
9. Labad, F.; Jurado, A.; Scheiber, L.; Teixidó, M.; Vázquez-Suñé, E.; Pérez, S. Identifying Sources and Environmental Risks of Emerging Mobile Organic Pollutants in the Urban Groundwater of Barcelona (Spain). *Environ. Chem. Ecotoxicol.* **2025**, *7*, 1922–1932. https://doi.org/10.1016/j.enceco.2025.08.017.
10. Riedel, T.; Piepenbrock, A.; Schertzinger, G.; Weitzel, I. Urban Groundwater Quality: A Comprehensive Survey of Emerging Pollutants below a Medium-Sized European City. *Grund. Z. Der Fachsekt. Hydrogeol.* **2026**, *31*, 73–88. https://doi.org/10.1007/s00767-025-00604-0.
11. Schirmer, M.; Leschik, S.; Musolff, A. Current Research in Urban Hydrogeology—A Review. *Adv. Water Resour.* **2013**, *51*, 280–291. https://doi.org/10.1016/j.advwatres.2012.06.015.
12. Mester, T.; Balla, D.; Karancsi, G.; Bessenyei, É.; Szabó, G. Effects of Nitrogen Loading from Domestic Wastewater on Groundwater Quality. *Water SA* **2019**, *45*, 349–358. https://doi.org/10.17159/wsa/2019.v45.i3.6731.
13. Rahim, F.B.; Swarnokar, S.C.; Roy, S.; Rahman, M.M.; Das, T.K. The Quality of Groundwater in Shallow Aquifers Impacted by Inadequately Managed Sanitation Facilities in Coastal Bangladesh. *Clean. Water* **2025**, *4*, 100154. https://doi.org/10.1016/j.clwat.2025.100154.
14. Wilschnack, K.; Cartmell, E.; Yates, K.; Petrie, B. Septic Tanks as a Pathway for Emerging Contaminants to the Aquatic Environment–Need for Alternative Rural Wastewater Treatment? *Environ. Pollut.* **2024**, *362*, 124988. https://doi.org/10.1016/j.envpol.2024.124988.
15. Robertson, W.D.; Van Stempvoort, D.R.; Schiff, S.L. Review of Phosphorus Attenuation in Groundwater Plumes from 24 Septic Systems. *Sci. Total Environ.* **2019**, *692*, 640–652. https://doi.org/10.1016/j.scitotenv.2019.07.198.
16. Nguyen, H.H.; Venohr, M. Harmonized Assessment of Nutrient Pollution from Urban Systems Including Losses from Sewer Exfiltration: A Case Study in Germany. *Environ. Sci. Pollut. Res.* **2021**, *28*, 63878–63893. https://doi.org/10.1007/s11356-021-12440-9.
17. Mester, T.; Szabó, G.; Kiss, E.; Balla, D. Long-Term Spatiotemporal Changes in Nitrate Contamination of Municipal Groundwater Resources after Sewerage Network Construction in the Hungarian Great Plain. *Environ. Sci. Pollut. Res.* **2024**, *31*, 61114–61137. https://doi.org/10.1007/s11356-024-35280-9.
18. Chlost, I.; Chmiel, S.; Cieśliński, R.; Fac-Beneda, J.; Kirvel, I.; Olszewska, A. Groundwater Springs in Young Glacial Areas and Their Role in Sustainable Environmental Development (Case Study—North Poland). *Sustainability* **2026**, *18*, 5245. https://doi.org/10.3390/su18115245.
19. Dąbrowska, D.; Rykała, W. Chemical Composition of Leachates from Municipal Waste Landfills in Southern Poland. *Pol. Hyperb. Res. ONL* **2026**, *96*, 121–129. https://doi.org/10.2478/phr-2026-0019.
20. Petruța, N.-L.; Sur, I.M.; Rusu, T.A.; Gabor, T.; Rusu, T. Integrated Assessment of Groundwater Vulnerability and Drinking Water Quality in Rural Wells: Case Study from Ceanu Mare Commune, Northern Transylvanian Basin, Romania. *Sustainability* **2025**, *17*, 6530. https://doi.org/10.3390/su17146530.
21. Annan, S.T.; Frimpong, B.; Owusu-Fordjour, C.; Boasu, B.Y. Assessing Localized Contamination Hazard and Groundwater Quality Challenges in Water-Stressed Peri-Urban Accra, Ghana. *J. Geosci. Environ. Prot.* **2022**, *10*, 13–28. https://doi.org/10.4236/gep.2022.101002.
22. Hirata, R.; Cagnon, F.; Bernice, A.; Maldaner, C.H.; Galvão, P.; Marques, C.; Terada, R.; Varnier, C.; Ryan, M.C.; Bertolo, R. Nitrate Contamination in Brazilian Urban Aquifers: A Tenacious Problem. *Water* **2020**, *12*, 2709. https://doi.org/10.3390/w12102709.
23. Dragon, K. Groundwater Nitrate Pollution in the Recharge Zone of a Regional Quaternary Flow System (Wielkopolska Region, Poland). *Environ. Earth Sci.* **2013**, *68*, 2099–2109. https://doi.org/10.1007/s12665-012-1895-5.
24. Mester, T.; Szabó, G.; Kiss, E.; Balla, D. Towards Environmental Sustainability: Wastewater Management and Sewer Networks for Protecting Groundwater in Rural Settlements. *Urban Sci.* **2025**, *9*, 80. https://doi.org/10.3390/urbansci9030080.
25. Saraswati, S.P.; Anggraeni, S.M.; Asriningtyas, V.; Permana, M.S.R.; Ahmad, J.S.M. Oxidation-Reduction Potential in Conjunction with Dissolved Oxygen in Bulaksumur Residence Greywater Treatment System. *IOP Conf. Ser. Earth Environ. Sci.* **2026**, *1593*, 012046. https://doi.org/10.1088/1755-1315/1593/1/012046.

26. Zhao, L.; Zhan, L.; Zhang, H.; Zhang, Y.; Wu, L.; Zhao, R.; Zheng, L.; Zhang, G. Tracking Groundwater Pollution Plumes at Landfill Sites Using Borehole Hydrochemical and Hydrodynamic Profile (BHHP) Method. *J. Environ. Manag.* **2023**, *345*, 118860. https://doi.org/10.1016/j.jenvman.2023.118860.
27. Venkata Ratnalu, G.; Dhakate, R.; More, S. Aqueous Geochemistry and Non-Carcinogenic Health Risk through Chloride and Nitrate Enriched Groundwater of Cosmopolitan Bangalore City, India. *Int. J. Environ. Anal. Chem.* **2023**, *104*, 7383–7407. https://doi.org/10.1080/03067319.2023.2173007.
28. Laoufi, A.; Guettaia, S.; Boudjema, A.; Derdour, A.; Almalki, A.S.; Bojer, A.K.; El-Nagdy, K.A.; Ali, E. Seasonal Groundwater Quality Analysis in a Drought Prone Agricultural Region Using GIS and IWQI for Nitrate Contamination Insights. *Sci. Rep.* **2025**, *15*, 22948. https://doi.org/10.1038/s41598-025-06884-z.
29. Katz, B.G.; Eberts, S.M.; Kauffman, L.J. Using Cl/Br Ratios and Other Indicators to Assess Potential Impacts on Groundwater Quality from Septic Systems: A Review and Examples from Principal Aquifers in the United States. *J. Hydrol.* **2011**, *397*, 151–166. https://doi.org/10.1016/j.jhydrol.2010.11.017.
30. McArthur, J.M.; Sikdar, P.K.; Hoque, M.A.; Ghosal, U. Waste-Water Impacts on Groundwater: Cl/Br Ratios and Implications for Arsenic Pollution of Groundwater in the Bengal Basin and Red River Basin, Vietnam. *Sci. Total Environ.* **2012**, *437*, 390–402. https://doi.org/10.1016/j.scitotenv.2012.07.068.
31. Tóth, T.; Kuti, L.; Kabos, L.; Pásztor, L. Use of Digitalized Hydrogeological Maps for Evaluation of Salt-Affected Soils of Large Areas. *Arid. Land Res. Manag.* **2001**, *15*, 329–346. https://doi.org/10.1080/153249801753127624.
32. van de Craats, D.; van der Zee, S.E.A.T.M.; Sui, C.; van Asten, P.J.A.; Cornelissen, P.; Leijnse, A. Soil Sodicity Originating from Marginal Groundwater. *Vadose Zone J.* **2020**, *19*, e20010. https://doi.org/10.1002/vzj2.20010.
33. Rajmohan, N.; Masoud, M.H.Z.; Niyazi, B.A.M. Impact of Evaporation on Groundwater Salinity in the Arid Coastal Aquifer, Western Saudi Arabia. *CATENA* **2021**, *196*, 104864. https://doi.org/10.1016/j.catena.2020.104864.
34. Vasvári, M.; Kovács, T. *Átalakuló Kisújszállás—Egy Nagykun Kisváros Társadalmi Folyamatai A 21. Században*; Debreceni Egyetemi Kiadó—Debrecen University Press: Debrecen, Hungary, 2026; ISBN 978-963-615-468-4.
35. Dövényi, Z.; Ambrózy, P.; Juhász, Á.; Marosi, S.; Mezősi, G.; Michalkó, G.; Somogyi, S.; Szalai, Z.; Tiner, T. Magyarország Kistájainak Katasztere = Inventory of Microregions in Hungary. Available online: http://real.mtak.hu/1416/ (accessed on 22 November 2026).
36. Terv, T.; Terv, T. *Settlement Structure Plan of Kisújszállás, 2012–2015*; CÍVIS TERV Urban Planning and Architectural Design Office Limited Partnership: Debrecen, Hungary, 2026. Available online: https://kisujszallas.smartonkormanyzat.hu/data-files/userfiles/files/Szerkterv_2025_M6_mod_egybeszerkesztett_Kisujszallas.pdf (accessed on 22 November 2026).
37. Mezősi, G. Physical Geography of the Great Hungarian Plain. In *The Physical Geography of Hungary*; Mezősi, G., Ed.; Springer International Publishing: Cham, Switzerland, 2017; pp. 195–229, ISBN 978-3-319-45183-1.
38. *HS ISO 7150-1:1992*; Determination of Ammonium in Water: Manual Spectrophotometric Method. Hungarian Standards Institution: Budapest, Hungary, 1992.
39. *HS 1484-13:2009*; Determination of Nitrate and Nitrite Content by Spectrophotometric Method. Hungarian Standards Institution: Budapest, Hungary, 2009.
40. *HS 448-18:2009*; Drinking Water Analysis—Part 18: Determination of Orthophosphate and Total Phosphorus Using Spectrophotometric Method. Hungarian Standards Institution: Budapest, Hungary, 2009.
41. *HS 448-20:1990*; Drinking Water Analysis—Determination of Chemical Oxygen Demand by the Potassium Permanganate Method. Hungarian Standards Institution: Budapest, Hungary, 1990.
42. *HS 1484-15:2009*; Water Quality—Part 15: Determination of Chloride Content by Argentometric Titration. Hungarian Standards Institution: Budapest, Hungary, 2009.
43. *HS 448-11:1986*; Drinking Water Analysis—Determination of Alkalinity by Titration and Calculation of Hydrogen Carbonate, Carbonate and Hydroxide Ion Content. Hungarian Standards Institution: Budapest, Hungary, 1986.
44. Ren, J.; Han, G.; Liu, X.; Gao, X.; Zhang, S. Unraveling Nitrate Source Dynamics in Megacity Rivers Using an Integrated Machine Learning–Bayesian Isotope Framework. *Water* **2026**, *18*, 106. https://doi.org/10.3390/w18010106.
45. Cao, S.; Li, Y.; Hao, Q.; Liu, C.; Zhu, Y.; Li, Z.; Yuan, R. Spatio-Temporal Analysis of the Sources and Transformations of Anthropogenic Nitrogen in a Highly Degraded Coastal Basin in Southeast China. *Environ. Sci. Pollut. Res.* **2023**, *30*, 86202–86217. https://doi.org/10.1007/s11356-023-28360-9.
46. Shepard, D. A Two-Dimensional Interpolation Function for Irregularly-Spaced Data. In *Proceedings of the 1968 23rd ACM National Conference*; Association for Computing Machinery: New York, NY, USA, 1968; pp. 517–524.

47. Biddau, R.; Dore, E.; Da Pelo, S.; Lorrai, M.; Botti, P.; Testa, M.; Cidu, R. Geochemistry, Stable Isotopes and Statistic Tools to Estimate Threshold and Source of Nitrate in Groundwater (Sardinia, Italy). *Water Res.* **2023**, *232*, 119663. https://doi.org/10.1016/j.watres.2023.119663.
48. Aleku, D.L.; Dähnke, K.; Pichler, T. Source, Transport, and Fate of Nitrate in Shallow Groundwater in the Eastern Niger Delta. *Environ. Sci. Pollut. Res.* **2024**, *31*, 65034–65050. https://doi.org/10.1007/s11356-024-35499-6.
49. Wei, X.; Zhou, Y.; Ran, L.; Chen, M.; Zou, J.; Fan, Z.; Fu, Y. Sources and Transformation of Nitrate in Shallow Groundwater in the Three Gorges Reservoir Area: Hydrogeochemistry and Isotopes. *Water* **2024**, *16*, 3299. https://doi.org/10.3390/w16223299.
50. Martinelli, G.; Dadomo, A.; De Luca, D.A.; Mazzola, M.; Lasagna, M.; Pennisi, M.; Pilla, G.; Sacchi, E.; Saccon, P. Nitrate Sources, Accumulation and Reduction in Groundwater from Northern Italy: Insights Provided by a Nitrate and Boron Isotopic Database. *Appl. Geochem.* **2018**, *91*, 23–35. https://doi.org/10.1016/j.apgeochem.2018.01.011.
51. Tóth, T.; Pásztor, L.; Kabos, S.; Kuti, L. Statistical Prediction of the Presence of Salt-Affected Soils by Using Digitalized Hydrogeological Maps. *Arid. Land Res. Manag.* **2002**, *16*, 55–68. https://doi.org/10.1080/153249802753365322.
52. Bakacsi, Z.; Tóth, T.; Makó, A.; Barna, G.; Laborczi, A.; Szabó, J.; Szatmári, G.; Pásztor, L. National Level Assessment of Soil Salinization and Structural Degradation Risks under Irrigation. *Hung. Geogr. Bull.* **2019**, *68*, 141–156. https://doi.org/10.15201/hungeobull.68.2.3.
53. Gulgundi, M.S.; Shetty, A. Groundwater Quality Assessment of Urban Bengaluru Using Multivariate Statistical Techniques. *Appl. Water Sci.* **2018**, *8*, 43. https://doi.org/10.1007/s13201-018-0684-z.
54. Mohammed, M.A.A.; Szabó, N.P.; Mikita, V.; Szűcs, P. Tracking the Spatiotemporal Evolution of Groundwater Chemistry in the Quaternary Aquifer System of Debrecen Area, Hungary: Integration of Classical and Unsupervised Learning Methods. *Environ. Sci. Pollut. Res.* **2025**, *32*, 6884–6903. https://doi.org/10.1007/s11356-025-36175-z.
55. He, Y.; Duan, Z.-L.; Ding, X.-H.; Zhang, Z.; Mayoulou, R.E.; Zhu, K.-F. Spatiotemporal Prediction for Groundwater Heavy Metal Contamination Using Soft-DTW-Based Clustering and Graph Neural Network Framework. *Water Res.* **2026**, *291*, 125245. https://doi.org/10.1016/j.watres.2025.125245.
56. Ding, X.-H.; Luo, B.; Zhou, H.-T.; Chen, Y.-H. Generalized Solutions for Advection–Dispersion Transport Equations Subject to Time- and Space-Dependent Internal and Boundary Sources. *Comput. Geotech.* **2025**, *178*, 106944. https://doi.org/10.1016/j.compgeo.2024.106944.


**Disclaimer/Publisher's Note:** The statements, opinions and data contained in all publications are solely those of the individual author(s) and contributor(s) and not of MDPI and/or the editor(s). MDPI and/or the editor(s) disclaim responsibility for any injury to people or property resulting from any ideas, methods, instructions or products referred to in the content.